Dolfi *et al. EvoDevo* (2019) 10:29
https://doi.org/10.1186/s13227-019-0142-5

EvoDevo

RESEARCH Open Access

Cell cycle dynamics during diapause entry and exit in an annual killifish revealed by FUCCI technology

Luca Dolfi[1], Roberto Ripa[2,4], Adam Antebi[1], Dario Riccardo Valenzano[1] and Alessandro Cellerino[2,3*]

Abstract

Background: Annual killifishes are adapted to surviving and reproducing over alternating dry and wet seasons. During the dry season, all adults die and desiccation-resistant embryos remain encased in dry mud for months or years in a state of diapause where their development is halted in anticipation of the months that have to elapse before their habitats are flooded again. Embryonic development of annual killifishes deviates from canonical teleost development. Epiblast cells disperse during epiboly, and a "dispersed phase" precedes gastrulation. In addition, annual fish have the ability to enter diapause and block embryonic development at the dispersed phase (diapause I), mid-somitogenesis (diapause II) and the final phase of development (diapause III). Developmental transitions associated with diapause entry and exit can be linked with cell cycle events. Here we set to image this transition in living embryos.

Results: To visibly explore cell cycle dynamics during killifish development in depth, we created a stable transgenic line in *Nothobranchius furzeri* that expresses two fluorescent reporters, one for the G_1 phase and one for the S/G_2 phases of the cell cycle, respectively (Fluorescent Ubiquitination-based Cell Cycle Indicator, FUCCI). Using this tool, we observed that, during epiboly, epiblast cells progressively become quiescent and exit the cell cycle. All embryos transit through a phase where dispersed cells migrate, without showing any mitotic activity, possibly blocked in the G_1 phase (diapause I). Thereafter, exit from diapause I is synchronous and cells enter directly into the S phase without transiting through G_1. The developmental trajectories of embryos entering diapause and of those that continue to develop are different. In particular, embryos entering diapause have reduced growth along the medio-lateral axis. Finally, exit from diapause II is synchronous for all cells and is characterized by a burst of mitotic activity and growth along the medio-lateral axis such that, by the end of this phase, the morphology of the embryos is identical to that of direct-developing embryos.

Conclusions: Our study reveals surprising levels of coordination of cellular dynamics during diapause and provides a reference framework for further developmental analyses of this remarkable developmental quiescent state.

Background

Annual killifishes inhabit temporary habitats that are subject to periodic desiccations [1]. In order to survive these extreme conditions, their eggs are laid in the soft substrate and remain encased in the dry mud where they are relatively protected from desiccation and can survive for prolonged periods during the dry season and regulate their development in anticipation of the ensuing rainy season. When their habitats are flooded, these embryos hatch, grow and mature rapidly and spawn the next generation before water evaporates [2–6]. This seasonal life cycle comprising embryonic arrest is widespread in arthropods from temperate climates, but it is unique among vertebrates.

As an adaptation to seasonal water availability, embryonic development of annual killifishes deviates from canonical teleost development for three main distinctive traits. The first is a slow cell cycle during early cleavage.

*Correspondence: alessandro.cellerino@sns.it
[2] Bio@SNS, Scuola Normale Superiore, Pisa, Italy
Full list of author information is available at the end of the article

While embryos of non-annual teleost fishes execute one cell division every 15–30 min during the first divisions after fertilization, the rate of early cell division in annual killifishes can reach almost 2 h [7]. As a result, an annual killifish embryo can be still in the blastula stage, while a non-annual killifish embryo fertilized at the same time has started somitogenesis.

The second trait is the dispersion of epiblast cells during epiboly and a decoupling between epiboly and gastrulation. When epiboly starts, the epiblast cells delaminate, assume an amoeboid shape and migrate towards the other pole of the egg. This migration is physically guided by the spreading of the extra embryonic enveloping layer [8]. In annual killifishes, the embryo at the end of epiboly consists only of extraembryonic structures and separated epiblast cells that migrate randomly over the yolk surface in a unique developmental stage named dispersed phase [6]. The dispersed phase can last for several days, and the embryonic axis is formed by migration of the epiblast cells towards a point where they reaggregate and form the embryonic primordium. This peculiar stage is named reaggregation phase [6]. In several teleosts, including zebrafish, gastrulation and axis formation take place during epiboly. However, in annual killifishes the formation of the three embryonic layers, which happens during gastrulation, takes place after epiboly during the late aggregation phase as demonstrated by live cell imaging and by the expression of the blastopore markers *goosecoid* and *brachyury* [9].

The third unique feature of annual killifish development is the ability to enter diapause. Diapause is a state of dormancy that retards or blocks embryonic development in anticipation of predictable cyclic hostile conditions. Diapause is widespread among arthropods from temperate climates that spend in diapause the coldest part of the year. Annual killifish embryo can arrest in diapause in three specific phases of development: during the dispersed phase (diapause I), at mid-somitogenesis when most organs are formed (diapause II) or at the final stage of development (diapause III) [4]. Duration of diapause is highly variable, and diapauses are not obligatory [4]. These adaptations are interpreted as bet-hedging strategies that ensure survival in an unpredictable environment, which are typical of seed banks [3, 10]. Under appropriate conditions, such as high temperature or under the influence of maternal factors, embryos can greatly shorten and possibly skip all three diapauses and proceed through direct development [11–14]. Diapause II is not a simply a phase of developmental arrest, but direct development and diapause are alternative developmental trajectories, characterized by different morphologies. In particular, during somitogenesis, the embryos committed to diapause II grow in the longitudinal direction but are impaired in transversal growth and therefore have reduced transversal diameter of head and body as compared to direct development embryos [13, 15]. This difference is detectable already at the start of somitogenesis, and it is observed in multiple independent clades that have evolved diapause [15] and can have an impact on post-hatch life-history traits [10].

One species of annual killifish has recently become a relatively widespread experimental model: *Nothobranchius furzeri*. This is the shortest-lived vertebrate that can be cultured in captivity, and it replicates many typical phenotypes of vertebrate and human ageing [2, 16–18]. For this reason, it has been used as an experimental model to investigate the effects of several experimental manipulations on ageing [10, 19–25]. Natural habitats of this species can last as short as a month [26, 27] and yet are able to sustain a viable population since sexual maturity can be reached within 2 weeks from hatching [28]. This implies that embryos remain blocked in diapause for several months or even years, as a safe mechanism to prevent species eradication in the case of a drought year. Our personal observations (AC, DRV) show that also in captivity some *N. furzeri* eggs can remain in diapause II for more than a year. *N. furzeri* therefore represent an extreme case of compressed lifespan among annual killifishes and in natural conditions it spends longer time as embryos in diapause than in post-hatch stages.

Molecular studies of killifish embryonic development are scarce. It is known that diapause II is characterized by reduced protein synthesis, cell cycle arrest and remodelling of mitochondrial physiology, and it is controlled by insulin-like growth factor 1 signalling [29–35]. Recently, RNA-seq studies have shown that gene expression patterns during diapause resemble those observed during ageing [36] and vitamin D signalling controls to the choice between direct development and diapause II [37]. While early embryonic development following fertilization has been in part studied [7–9], the characterization of the physiological and molecular events occurring during diapause I has been started to be investigated only recently [35, 38, 39]. Here, to investigate entry and exit form diapause I and II, we created a stable transgenic line in *N. furzeri* that expresses genetically encoded fluorescent reporters for cell cycle phases using the Fluorescence Ubiquitination-based Cell Cycle Indicator (FUCCI) system that exploits the sequential degradation of fluorescent-tagged fragments of the cell cycle regulators Cdt1 and Geminin by the ubiquitin ligases SCF/Cdh1 and APC/C, respectively [40]. The APC/C is activated in late mitosis and stays active throughout G1 phase, while SCF/Skp2 is an APC/C target itself and thus can only become activated in S/G2 and early mitosis. The Azami-Green and Kusabira-Orange coding sequences were fused to

ubiquitination signals recognized by the APC/C and SCF/Cdh1, respectively. Because of the mutually exclusive activity of the two E3 ligases, the Cdt1-based sensor is only visible during G1 phase, while the Geminin-based sensor is only detectable during S/G2/M [40]. This tool enabled us to shed light on the cell cycle characteristics of cells during diapause I and to demonstrate that diapause exit is characterized by rapid and synchronous cell cycle reactivation. These characteristics appear unique among vertebrate embryos.

Results and discussion

To identify a suitable promoter for FUCCI reporter lines, we tested the activity in *N. furzeri* of the zebrafish ubiquitin (ubi) promoter [41] using EGFP as reporter. We observed ubiquitous expression of the EGFP from the second day of development into adulthood in this Tg *ubi:egfp* line (Fig. 1f).

Two different FUCCI transgenic lines were successfully generated using the Tol2 transgenesis system [42–44]: (i) a "FUCCI green" reporter (Azami-Green—Geminin), which is activated during the S/G2/M phase of the cell cycle [40] and (ii) a "FUCCI red" reporter (Kusabira-Orange—Cdt1), which is activated during the G1 phase of the cell cycle [40]. Since the original FUCCI construct is not functional in zebrafish, these constructs were previously modified using sequences from the zebrafish ortholog of Cdt1 and Gemin [40]. We used these constructs without modifications. Both transgenes were placed under the control of the zebrafish *ubi* promoter (Fig. 1a, b), a ubiquitous promoter that drives transcription in all tissues at any developmental stage (Fig. 1e, f).

Adult F0 transgenic fish were screened for fluorescence and bred one to another. F1 fish showing the expected fluorescence pattern were interbred in order to increase the number copies of FUCCI reporter cassettes in their genome, thereby enhancing the fluorescence signal in the F2 generation (Fig. 1c). F2 transgenic fish were used to characterize the expression pattern of the FUCCI reporters at different developmental stages.

To confirm that red fluorescence labels cells in the G0/G1 phase and green fluorescence labels cells in the S/G2/M phase (Fig. 1d), we performed FACS analysis on newly hatched embryos and on adult testis that represent a highly mitotic organ. We could differentiate four types of cells: "black" cells, devoid of fluorescence, red fluorescent cells, green fluorescent cells and double-labelled cells. Analysis of DNA content in these four different types of cells clearly showed that "dark" and red fluorescent cells correspond to G0/G1, green fluorescent cells correspond to S phase and double-labelled cells showed higher DNA content that green fluorescent cells, indicating that they were in G2 phase (Fig. 1g). This phenomenon is expected since, because the APC/C E3 ligase is activated only during late mitosis and, if G2 is of sufficient length, the Cdt1 sensor can accumulate again in G2 phase, resulting in double-labelling of these cells.

We describe the expression pattern of the transgenes in two parts: the first part provides a general description of the fluorescent signal in the single lines (FUCCI green and FUCCI red, respectively) during focal stages of embryonic development and in adult life. The second part is focused on the double transgenic line, where both the red and green signals are present. In this part, changes in relative intensity of the two signals are described and interpreted with respect to the dynamic processes that characterize the different phases of killifish embryonic development.

Part 1

FUCCI red

The FUCCI red signal is localized in the nuclei of cells in every stage of *N. furzeri* life. During the dispersed phase (Fig. 2A, B), two cell types expressed red fluorescence: large cells of the enveloping layer (EVL) and some smaller

(See figure on next page.)

Fig. 1 FUCCI transgenic line generation. **a**, **b** Schematic representations of FUCCI green and red constructs, respectively. FUCCI constructs were injected separately in different 1-cell stage fertilized eggs. Positive eggs were raised into adult fish, bred and screened for three generations (**c**). F2 FUCCI green fish were finally bred with F2 FUCCI red fish to generate double FUCCI embryos, which were used for most experiments (**c**). **d** Schematic representation of how FUCCI technology works, cells are green during S/G2/M phases, colourless between M and G1, red in G1 and G0 phases and yellow during a small portion of G2 phase. **e** Schematic representation of zUbiquitin-EGFP construct. EGFP expression driven by zUbiquitin promoter in Nothobranchius embryos and adult fish is shown (**f**). **g** FACS analysis of double FUCCI embryo. The scatterplot on the left shows the gating used to separate the four cell populations. The numbers indicate the percentage of cells in the four populations. The middle graph represents the intensity of the Hoechst staining as measure of DNA content of the four different populations. The graph on the right is the same as the graph in the middle but population are normalized on their own cells count rather than the total cells count. **h** FACS analysis of adult gonads of double FUCCI fish. The scatterplot on the left shows the gating used to separate the four cell populations. The numbers indicate the percentage of cells in the four populations. The middle graph represents the intensity of the Hoechst staining as measure of DNA content of the four different populations. The graph on the right is the same as the graph in the middle but population are normalized on their own cells count rather than the total cells count

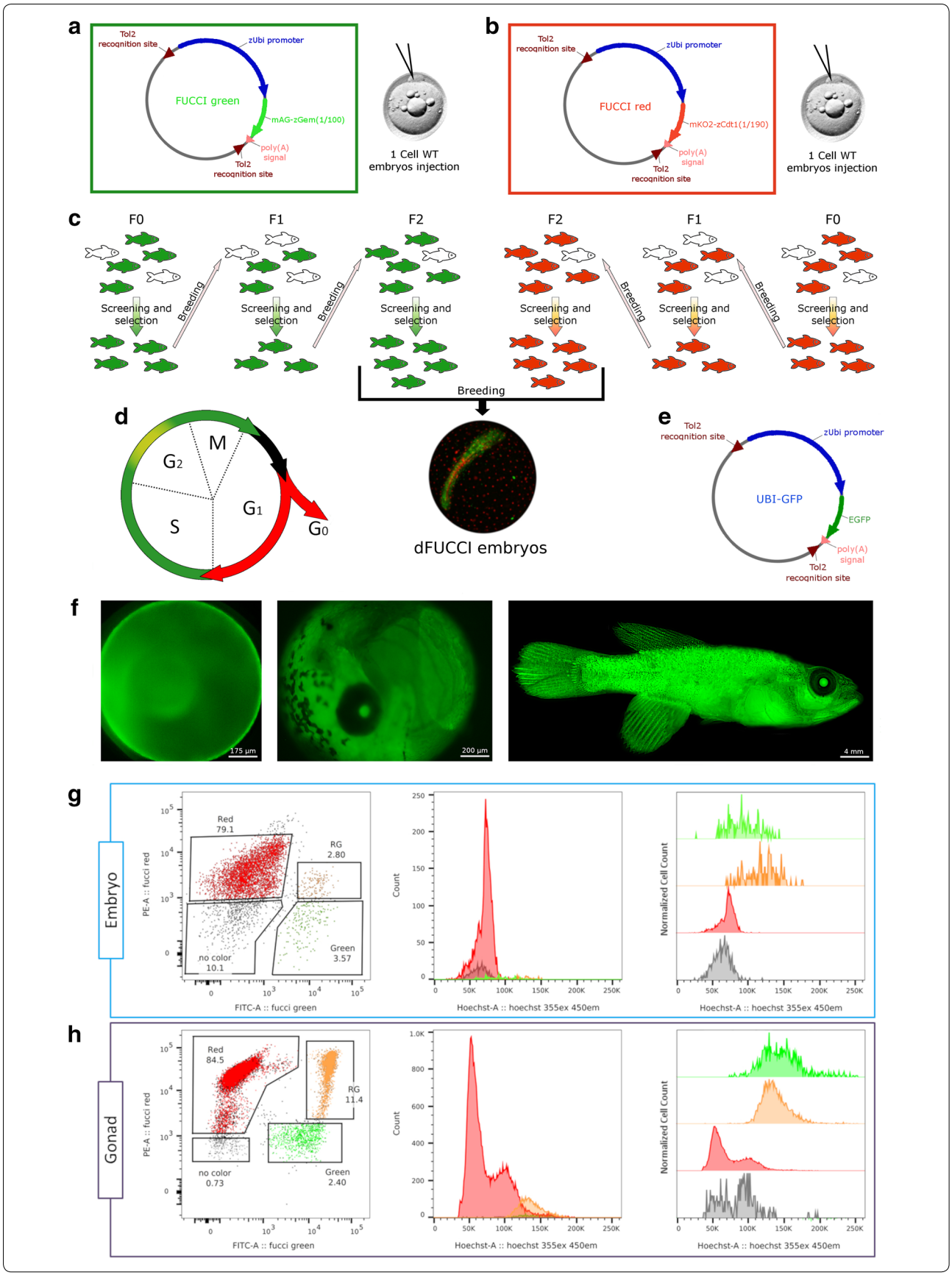
a
Tol2 recognition site
zUbi promoter
FUCCI green
mAG-zGem(1/100)
poly(A) signal
Tol2 recognition site
1 Cell WT embryos injection
b
Tol2 recognition site
zUbi promoter
FUCCI red
mKO2-zCdt1(1/190)
poly(A) signal
Tol2 recognition site
1 Cell WT embryos injection
c
F0
F1
F2
F2
F1
F0
Screening and selection
Breeding
Breeding
Breeding
Breeding
Breeding
d
G2
M
G1
S
G0
dFUCCI embryos
e
Tol2 recognition site
zUbi promoter
UBI-GFP
EGFP
poly(A) signal
Tol2 recognition site
f
175 µm
200 µm
4 mm
g
Embryo
Red 79.1
RG 2.80
Green 3.57
no color 10.1
PE-A :: fucci red
FITC-A :: fucci green
Count
Hoechst-A :: hoechst 355ex 450em
Normalized Cell Count
h
Gonad
Red 84.5
RG 11.4
Green 2.40
no color 0.73
PE-A :: fucci red
FITC-A :: fucci green
Count
Hoechst-A :: hoechst 355ex 450em
Normalized Cell Count

cells of the epiblast (Fig. 2C, arrows). The nuclei of EVL cells ranged from 22 to 27 μm in diameter and formed a regular array over the yolk surface. The nuclear diameter of epiblast cells was smaller, on the order of 7–9 μm. Both these cell types were red, but the epiblast cells were most likely in G1, since their fluorescence faded and increased over time course of hours, indicating that they were engaged in the cell cycle. By contrast, the EVL cells appeared to be in G0, since the red fluorescence never faded and lasted throughout embryonic development, until hatching.

At the somitogenesis stage (Fig. 2D, E), the regular distribution of the EVL cells remained unchanged. All the other red cells in the embryo showed a patterned distribution that was particularly striking in the embryo trunk, where the somites were clearly delineated (Fig. 2E, β). In the older more rostral somites (Fig. 2G), the inner part of the somites showed a high concentration of red cells, while in the more caudal part of the embryo (Fig. 2F)—where somites were still forming—the red cells were more spread and diffused. Once the new somite pair was completely formed, red cells increased in numbers, becoming more dense and localized in the inner part (Fig. 2G, stars), becoming constitutively red. Just below the notochord midline, another narrow streak of red cells extended from the tip of the head region to the tip of the tail (Fig. 2G, λ). Also, the head region contained several areas with red cells, but these were quite rare, spread out and did not demarcate specific areas (Fig. 2E, α).

Hatched fry had large fraction of red cells (Fig. 2H). The lateral muscles of the trunk (Fig. 2H, d) and of the tail (Fig. 2H, e) harboured a large number of red cells. In the head region, nearly every part of the brain had some spread red cells or red cells aggregates (Fig. 2H, a). The lens (Fig. 2H, b) showed strong red fluorescence at this stage. This could be an artefact due to the high protein stability in this region and lack of degradation of the FUCCI reporter. What remained of the yolk at this stage was still surrounded by large red cells belonging to the EVL, blocked in G0 and not cycling (Fig. 2H, f). Lastly, a large patch of red cells was observed corresponding to the pectoral fins (Fig. 2H, c).

The adult FUCCI red transgenic fish appeared completely red under fluorescence since many cells were in G0 or possibly G1 phase (Fig. 2I, J). Males and females showed a pattern that was virtually identical, and the signal intensity was comparable between different specimens (Fig. 2I, J).

FUCCI green

During the dispersed phase, different proportions of green epiblast cells were detected in different FUCCI green embryos belonging to the same clutch of eggs. The number of green nuclei observed varied between 20 (Fig. 2M, N) and 200 (Fig. 2K, L), with a size range between 7 and 25 μm in diameter, typically showing a higher amount of the smaller cells. During this developmental stage, cells arranged randomly over the yolk surface.

In developing embryos, during somitogenesis proliferating green cells were detected in every part of the forming embryos (Fig. 2O, P). The signal was moderately strong in the trunk, in the tail (Fig. 2P, β) and in the head primordia (Fig. 2P, α). The maximum intensity of the signal, i.e. the maximum density of proliferating cells, was limited to a narrow region along the midline, that extended from the end of the head to the end of the tail, between the yolk surface and the lowest part of the somites (Fig. 2Q, orange box, δ). Many green cells migrated over the yolk surface during all of somitogenesis.

In the hatched fry, the proliferative regions in the embryos were more defined. In the torso and the tail, green cells were spread out but homogeneously distributed (Fig. 2R, f). Slightly more dense green cells proliferated in the caudal and pectoral fins (Fig. 2R, d) and at the base of the head in the hindbrain (Fig. 2R, e). The optic tectum (Fig. 2R, a) showed a clear pattern with thick and dense aggregates of green cells at the borders, in the proliferating niches, with almost no green cells in the inner part, appearing completely dark. The olfactory bulb (Fig. 2R, b) in the fry was one of the major proliferating regions, composed by thick streaks of green cells. Lastly, the lens appeared green (Fig. 2R, c), but as for the FUCCI red transgenic line, this could be an artefact due to lack of degradation of the FUCCI reporter. In adults, no green cells could be detected with a stereomicroscope and the only green signal detectable was confined to the region of the eyes (Fig. 2S, T, arrow).

Part 2

F2 fish were crossed (FUCCI red with FUCCI green), generating double FUCCI green/red embryos (dFUCCI), which were analysed by means of time lapse confocal imaging. Embryos from this cross were imaged for periods spanning from hours to days at different stages of development from the end of epiboly to late somitogenesis, i.e. past the stage when embryos entered diapause II. The stacks of images of each time point were then processed with IMARIS software to perform particle tracking and counting.

These experiments required occupancy of the setup for considerable amounts of time, as every single time lapse acquisition lasted from 8 h to 4 days, limiting the number of replicates available for each stage (Table 1). This study was designed to provide an overview, as complete as

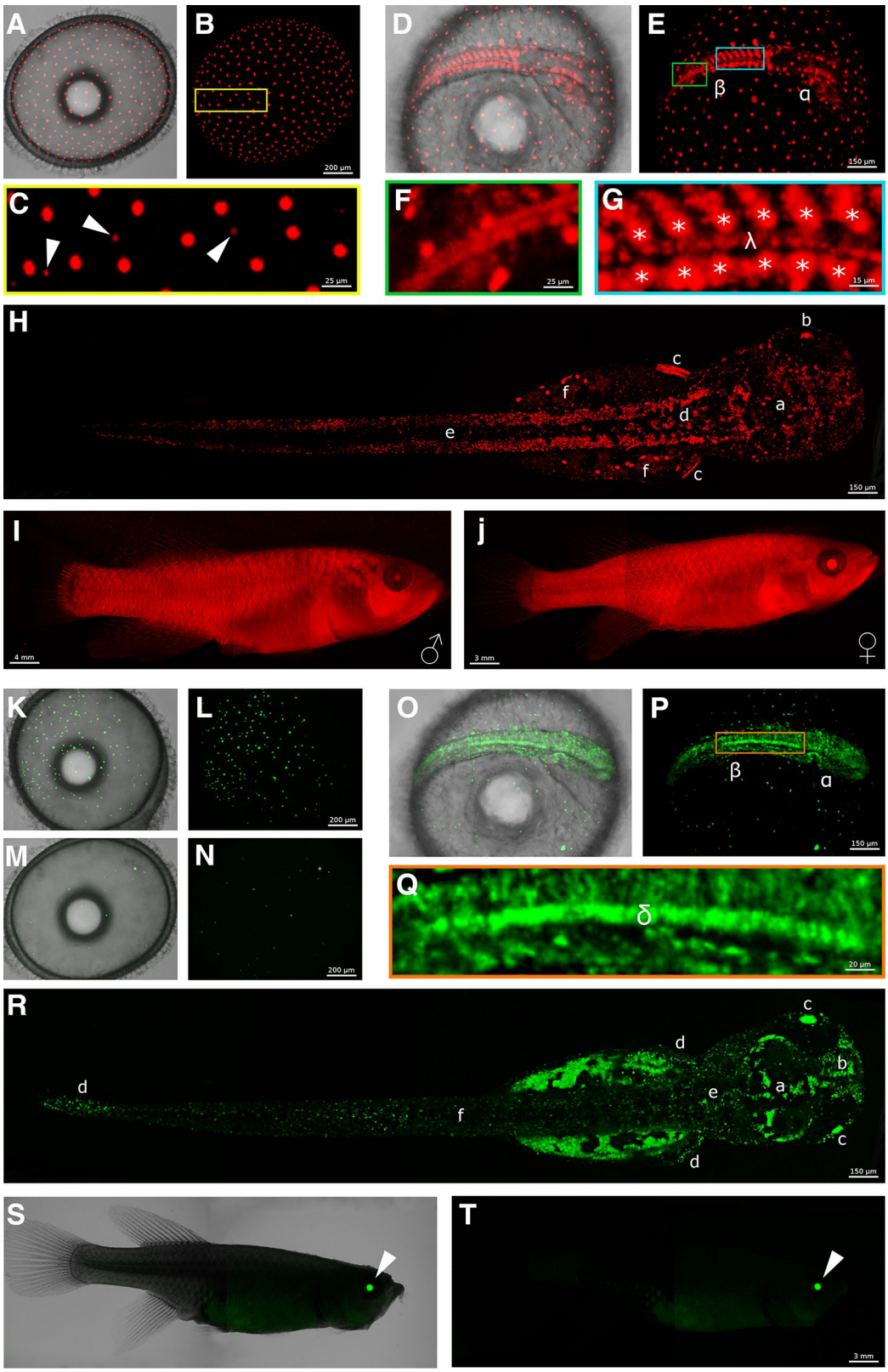

Fig. 2 FUCCI green and FUCCI red characterization. **A** to **J** show FUCCI red expression at different developmental stages. **K** to **T** show FUCCI green expression at different developmental stages. **A**–**C**, **K**–**N** dispersed phase. **D**–**G**, **O**–**Q** somitogenesis stage. **H**, **R** hatched fry. **I**, **J**, **S**, **T** adult fish. For a detailed description, see the main text

Table 1 Overview of dFUCCI embryos imaged for each developmental stage

Embryonic stage	Time required to reach the stage in *N. furzeri* at 28 °C	Stage duration at 28 °C	Amount of embryos imaged
Dispersed phase (WS 19–20)			
Early (small number of green cells)	4 days	1 to 30 days	4
Late (larger number of green cells)	7 days on average	12–24 h	6
Dispersed phase transition (from few to many green cells)	5–7 days on average	2–3 days	4
Reaggregation phase (WS 21–25)	8 days on average	8–12 h	4
Extension phase (WS 26)	9 days on average	8–12 h	4
Somitogenesis (without diapause II arrest) (WS 29–33)	10 days on average	5–8 days	6
Diapause II arrest and release	11 days on average	Days to years	4

It shows the number of embryos acquired at each developmental stage. From stage to stage, embryos acquired could be the same, acquired progressively during its development, or different ones. WS means Wourms' stage [12]

possible, of *N. furzeri* embryonic development (compromising on the number of replicates) as opposed to deep analysis of only one specific stage (e.g. reaggregation) with a larger number of replicates. Because the morphology of South American and African annual killifishes is comparable, we follow here the staging developed by Wourms for the South American annual killifish *Austrofundulus limnaeus* [6] for reference.

In his work, Wourms described the stages of killifish development from egg fertilization to fry. He dived the development in a total of 46 stages: 43 pre-hatching and three post-hatching. Stage 1 defines the freshly fertilized 1 cell stage embryo, while stage 46 describes the fry after digestion of the yolk that is starting to hunt prey.

In our work, we focus on a subset of these stages and, more precisely, we describe development from stage 19 to 33, which correspond to the phase between completion of epiboly and beginning of the dispersed phase to an advanced stage of somitogenesis.

End of epiboly (WS 19)

Detection of fluorescence signal with a confocal microscope was not possible before the stage of 70% epiboly because the expression of the fluorescent reporters was too weak: earlier stages of epiboly were described previously by injecting synthetic RNA coding for FUCCI reporters [7]. During epiboly, three cell layers become defined: the yolk syncytial layer (YSL), the enveloping layer (EVL) and the epiblast layer (EL) (Fig. 3).

Two of these three cell types could be clearly distinguished based on dFUCCI signal: the EVL cells and the EL cells, which could be distinguished based on their non-overlapping spans of nuclear sizes (21–27 µm vs. 8–12 µm, respectively). The EL cells (showing either green or red fluorescence) migrated in an apparently random direction in the space between the YSL and the EVL. Remarkably, these cells continued their movements also once epiboly was completed. Random movements of

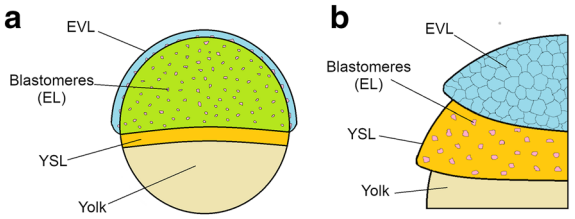

Fig. 3 Schematic representation of embryonic layers in annual killifish species. Yolk syncytial layer (YSL) is made of cell forming a syncytium and in direct contact with the yolk. On top of this layer migrate and divide the blastomeres, a discrete population of cell composing the epiblast layer. The enveloping layer (EVL) is the layer of cells on top, a thin layer that completely envelope the other two. Two representations are shown, a lateral semi-transparent view (**a**) and a cutaway representation (**b**)

EL cells in the dispersed phase were originally reported by Lesseps et al., in the 1970s [45] by means of bright-field microscopy and were later confirmed by us [6].

EVL cells maintained red fluorescence for the entire span of subsequent development, possibly indicating arrest in G_0 phase, which is coherent with the not proliferating status of these cells. Additionally, their number remained stable around 200 in the portion of the embryo that could be imaged (corresponding roughly to the superior pole) (Fig. 4). EVL cells showed a directional movement until the completion of epiboly (Wourms' stages 18–19) (Additional file 1: Movie S1), when they reached their final position and constituted a syncytium, which was then maintained during the ensuing development. This physical movement and positioning of EVL cells play an important role during the development of killifish embryos. The spreading of EL cells is indeed instructed by mechanical interactions between EVL and EL cells [8].

EVL cells formed a defined and regular architecture, tiling the entire surface at an average distance of about 80 µm from each other. Therefore, we used the position

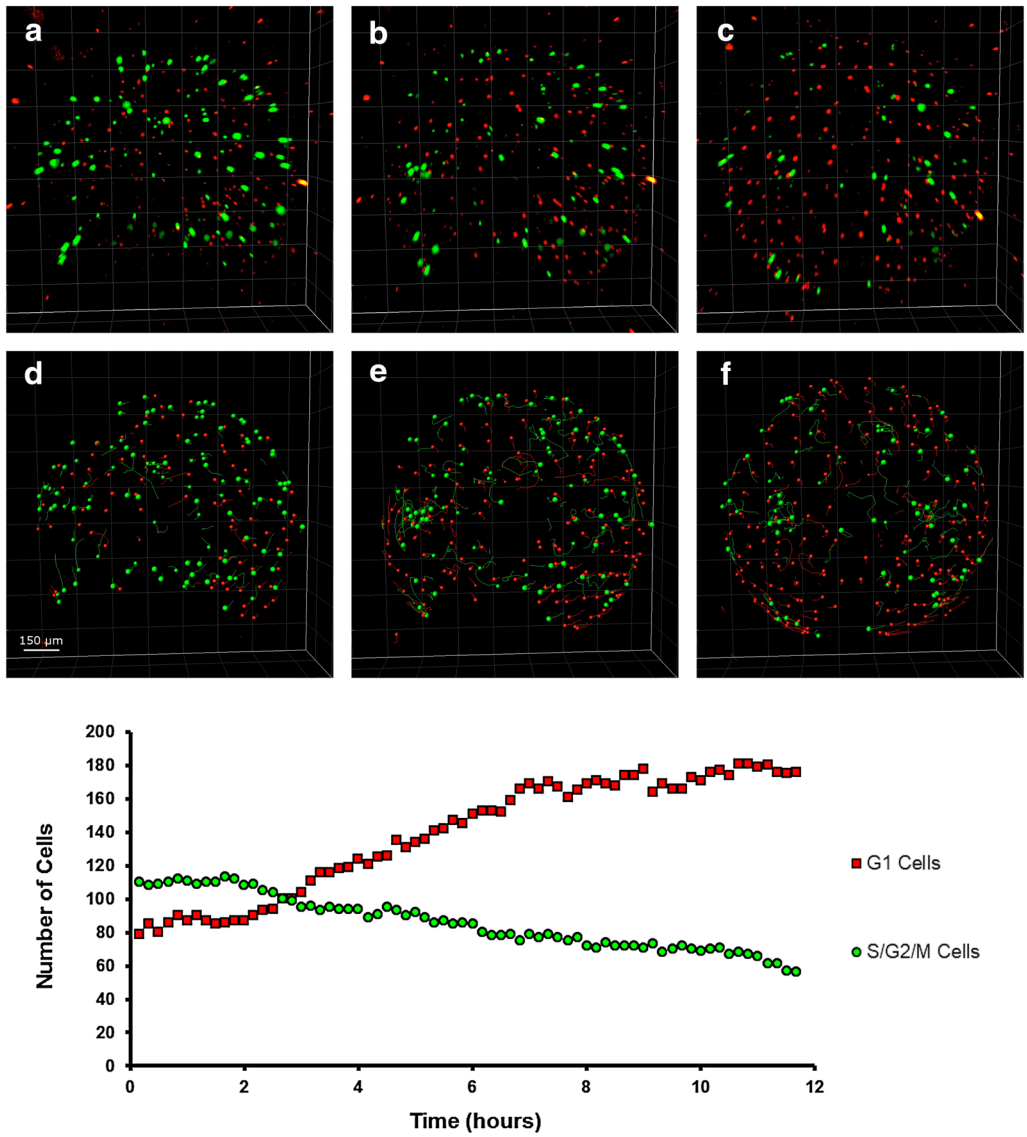

Fig. 4 Cell dynamics during epiboly (Wourms' stages 18–19). When epiboly is ongoing, both green and red cells are present in dFUCCI embryos (**a**). As long as epiboly proceeds (**b**, **c**) the number of green EL cells gradually and slowly decreases over time, while the number of red EVL cells increases until the reaching of a plateau (graph hours 7–12). The cells in the field of view were easily tracked and counted transforming the dots in particles with IMARIS (**d**–**f**). The images and graph refer to the acquired portion of the embryos, corresponding to the superior hemisphere

of these nuclei as a reference to correct for yolk movements that often occurred in the embryos during development, allowing for precise tracking of the movements of all the other cells and developing structures (Fig. 5).

Early dispersed phase (Wourms' stages 19–20) and diapause I

When epiboly ends and the dispersed phase begins, the number of detectable green and red EL cells was reduced from more than 200 to less than 70, in a ratio of almost 1:1 (Figs. 4 and 6c, left panel). These cells are actively moving in a seemingly random fashion (Fig. 6b, c, right panel). It is important to remark that the decline in green and red cells does not correspond to cell loss, as EL cells are clearly detected by bright-field microscopy at this stage (Additional file 2: Movie S2, min 0.53 to 1.10). Previous studies of early cleavages by means of injection of synthetic FUCCI mRNA [7] also reported a "dark phase" when neither red nor green fluorescence is detectable. The majority of EL cells appear to be locked in this "dark phase" during early dispersed stage. Based on FACS analysis of embryos in later stages of

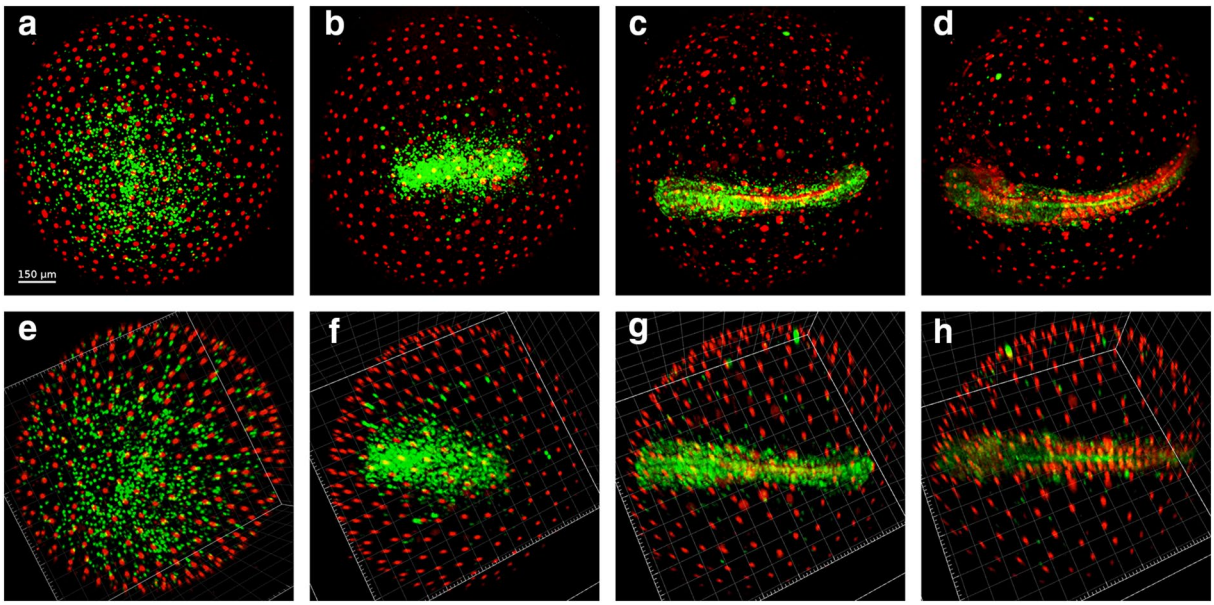

Fig. 5 ESL nuclei as reference point for drift correction. Embryos continuously move throughout development (**a**–**d**), but EVL nuclei do not move once they reach their final position at the end of epiboly. These nuclei can therefore be used as reference system and drifts and rotations that occur during development can be corrected using their position (**e**–**h**). Correcting the drifts allows a more precise and reliable cell tracking and data analysis

development (Fig. 1g, h), we should assume that these "invisible" cells are in G1 phase. A G1 block is indeed observed also in the South American killifish *A. limnaeus* [32].

In addition, all the embryos we could observe at the end of epiboly ($N > 30$, including embryos that were not followed in time lapse but only through still imaging) transited through a phase when only few EL green or red cells were detectable, characterized by the following features:

- Regularly spaced EVL large cells nuclei (19–25 µm nucleus diameter) that do not move, migrate or divide (Fig. 6).
- Presence of few (less than 80) red and green small epiblast cells (7–13 µm nuclear diameter) that do not divide (Fig. 6).
- Seemingly random cell movements, along with "dark" cells visible only in bright field (Additional file 2: Movie S2).

Early dispersal occurred in all embryos and was reached by a continuous decrease in green cells and an increase in red cells during epiboly (Fig. 4), leading finally to a stabilization of cells number (Fig. 6c). It has been recognized already in the 1970s that duration of early dispersal is variable (from hours to days); indeed, this stage corresponds to diapause 1 (DI) [4]. Noteworthy, DI is characterized by a complete stop of the cell cycle with cell possibly synchronized in G1 phase. However, DI is far from being a static stage, as cells constantly move over the yolk surface (Additional file 2: Movie S2, min 0.53 to 1.10). The functional relevance of erratic cell movements remains, for the moment, unexplored.

Synchronized cell cycle re-entry underlies release from diapause I

The mechanisms responsible for release from diapause I are unknown, although previous experiments suggest that it is a temperature-dependent process [14, 46, 47]. The majority of embryos imaged during dispersed phase were either in a phase with few green cells (80 or less) or in a phase with a larger number of green cells (300 or more), indicating that the duration of the transition is considerably shorter than either of these two phases and difficult to capture. We were nonetheless able to image the exit from DI in four embryos. In all four cases, the release from DI was characterized by the rapid appearance of a large number of green fluorescent cells that was not preceded by a rise in red cells, indicating that: (i) the "invisible" EL cells were indeed synchronized and (ii) most of the "invisible" EL cells, where both reporters are actively degraded, entered into $S/G_2/M$ phase without previous accumulation of the red reporter (Fig. 7). This indicates that either the transition is rapid or the

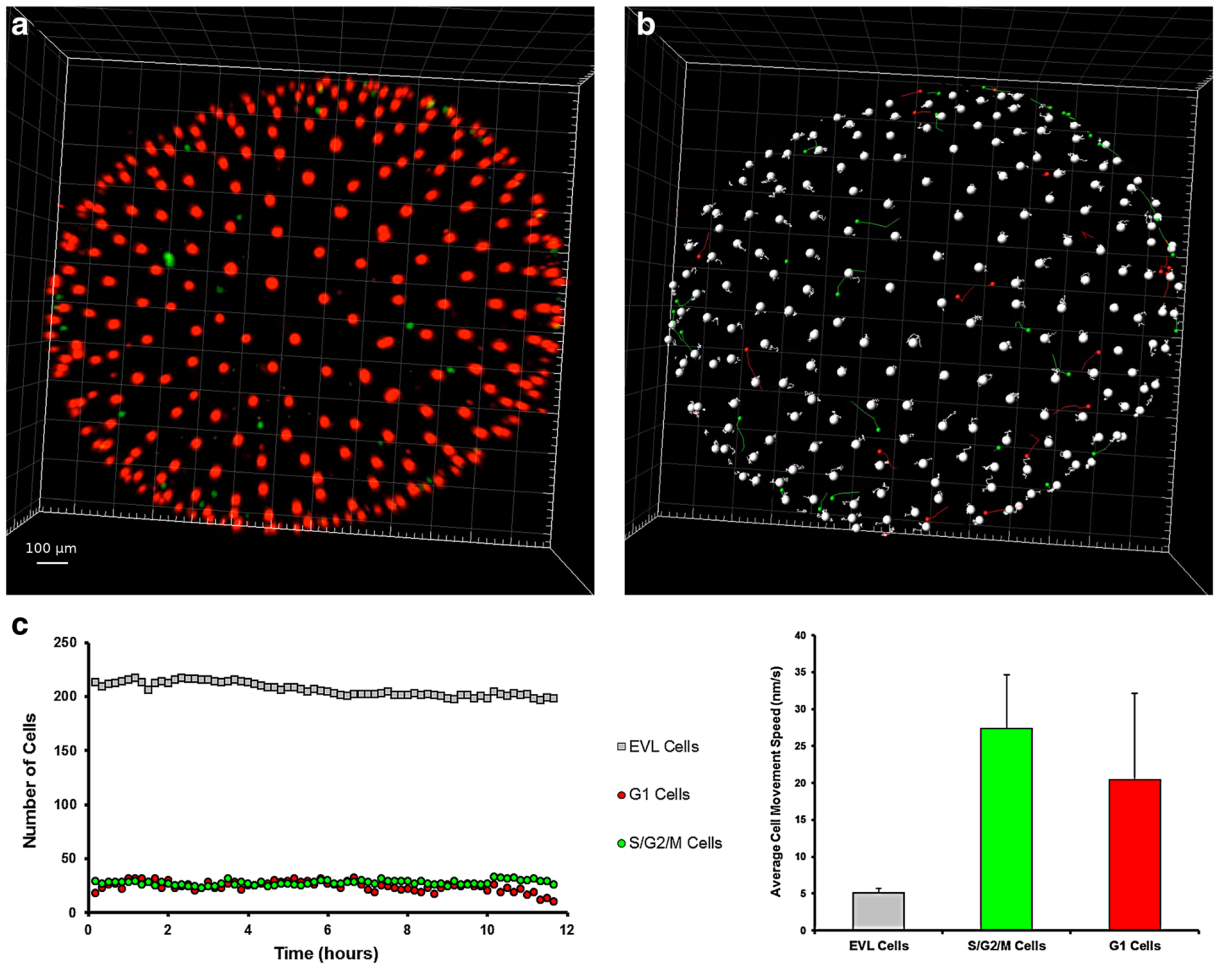

Fig. 6 Cell dynamics during the early dispersed phase (Wourms' stages 19–20). The first part of the dispersed phase is characterized by the presence of few EL green or red cells (**a**). ESL cells are pseudocoloured as large white dots and EL green and red cells as small green and red dots, respectively (**b**). Tracking of the three cell types over time. The number of each type of cell was constant for more than 10 h (**c**) and EL cells continuously moved during the whole time. Tracks of individual cells are shown in **b**, and speed average values in **c**, right panel. The images and graph refer to the acquired portion of the embryos, equivalent to the superior hemisphere

regulation of E3 ligases during diapause I differs from their regulation during the normal cell cycle. Remarkably, these reactivated cells showed what seemed to be a pattern of synchronous division, generating a peak of green cells followed by a period of reduced cell numbers (likely because some cells entered in the "dark" phase). In two out of the four imaged embryos, subsequent pulses with a periodicity of 10 h were apparent. Cells alternated from a green phase to a dark phase without showing a red phase, a pattern typical of early cleavage in *N. furzeri* [7]. Peaks of green fluorescent EL cells were present, but less apparent, in a third embryo whereas only the first peak was clearly visible in the fourth embryo (Additional file 3). This synchronization may simply reflect the fact that cells are synchronized during G1 and also cell cycle exit is synchronized. This is, however, a totally unique feature of embryonic development as cell cycle synchronization is otherwise known only for the very early phases of development that are controlled by maternal transcripts.

In all four cases, the number of cells increased over time—indicating active division—and the stage with ~ 300 green cells was reached in about 36 h. In addition, the proliferating cells moved erratically during the reactivation, in a way comparable to the movements of epiblast cells that were documented during DI by bright-field microscopy (Additional file 2) or during early dispersed phase by confocal microscopy (Fig. 4).